Supporting Information

$Cs_2VOF_4(IO_2F_2)$: Rationally Designing A Noncentrosymmetric Early-Transition-Metal Fluoroiodate

Mengmeng Ding[1], Hongping Wu[1], Zhanggui Hu[1], Jiyang Wang[1], Yicheng Wu[1] and Hongwei Yu[1*]

[1]*Tianjin Key Laboratory of Functional Crystal Materials, Institute of Functional Crystal, Tianjin University of Technology, Tianjin 300384, China*

To whom correspondence should be addressed: hwyu15@gmail.com

Experimental Section

Caution: *Hydrofluoric acid is toxic and corrosive! It must be handled with extreme caution and the appropriate protective equipment and training.*

Reagents.

Cesium fluoride (CsF, 99.9%, Tianjin hengshan Reagent), vanadium pentoxide (V_2O_5, 99.0%, Shanghai Ailan Reagent) and iodine pentoxide (I_2O_5, 98.0%, Shanghai Aladdin Reagent) were commercially available and used as received.

Hydrothermal Syntheses.

The crystals of title compound were synthesized by the hydrothermal method. The powder mixtures were prepared from CsF (0.5409 g, 3.56×10^{-3} mol), V_2O_5 (0.1619 g, 0.89×10^{-3} mol), I_2O_5 (0.2972 g, 0.89×10^{-3} mol), HF (0.5 mL) and H_2O (2 mL) with a Teflon liner (23 mL), and then sealed in an autoclave equipped. The autoclave was quickly heated to 220 °C for 72 hours, followed by slow cooling to 100 °C at a rate of 5 °C/h, subsequently cooled to room temperature by switching off the autoclave. The product was recovered by filtration and then dried in air. Thus, yellow crystals were obtained, and the yield of $Cs_2VOF_4(IO_2F_2)$ was 80% based on V_2O_5.

Powder X-ray Diffraction

The Powder X-ray diffraction (PXRD) patterns of $Cs_2VOF_4(IO_2F_2)$ was recorded on the SmartLab9KW X-ray diffractometer equipped with Cu K_α radiation at room temperature in the 2θ range of 10-70° with a step size of 0.02°. As seen in Figure S1, the experimental powder X-ray diffraction patterns are in agreement with the calculated pattern.

Single-Crystal X-ray Diffraction.

Single crystal X-ray diffraction experiments of title compounds at 296(2) K were performed on a Bruker SMART APEX II CCD with Mo−Kα radiation (λ = 0.71073 Å). The data were collected and integrated with the APEX II software. The structure was solved by using the SHELXTL system, and the structure's atomic positions were refined employing a full matrix least-squares technique.[1-2] The crystal data and structure refinement details are shown in Table S1 and the atomic coordination, atomic displacement parameters, selected bond lengths and angles are listed in Tables

S2 and S3.

Elemental Analysis.

Microprobe elemental analyses and the elemental distribution maps were performed using an energy dispersive X-ray spectroscope (EDS) with a field-emission scanning electron microscope (Quanta FEG 250) made by FEI.

UV-vis-NIR Diffuse Reflectance Spectroscopy

The UV-Vis-NIR diffuse reflectance spectrum of title compounds in 190–2500 nm wavelength range was performed on a Shimadzu SolidSpec-3700DUV spectrophotometer with $BaSO_4$ as a reference material at room temperature.

Infrared Spectroscopy

The Infrared (IR) spectrum of title compounds in 400–4000 cm^{-1} range was recorded on a Shimadzu IR Affinity spectrometer at room temperature.

Thermal Stability Measurement

The thermal properties of $Cs_2VOF_4(IO_2F_2)$ was measured on a NETZSCH STA 449C thermal analysis instrument. Powder samples (~10 mg) were placed in Al_2O_3 crucibles at a heating rate of 10 °C/min from 20 to 800 °C under flowing nitrogen gas.

Second-Order NLO Measurements.

The second-order NLO effects of $Cs_2VOF_4(IO_2F_2)$ was performed by employing the powder measurement method proposed by Kurtz−Perry.[3] Polycrystalline samples of $Cs_2VOF_4(IO_2F_2)$ was ground and then sieved them into six different standard sizes, as follows: 52–74, 74–100, 100–125, 125–150, 150–180 and 180–225 μm, and the KDP and KTP was considered as reference material.

The first-principles Calculations

The electronic structure of above crystals was carried out on the CASTEP package based on the plane-wave pseudopotential method.[4-5] The exchange and correlation functional was acquired by the Perdew−Burke−Ernzerhof (PBE) in the generalized gradient approximation (GGA), and the relationship between the ionic cores and the electrons was described by using norm-conserving pseudopotential.[6-7] The valence-electron configurations, Cs $5p^6 6s^1$, V $3p^6 3d^3 4s^2$, I $5s^2 5p^5$, O $2s^2 2p^4$, F $2s^2 2p^5$ were considered in the computation. The plane waves cutoff energy was set to 900 eV. And

the Monkhorst-Pack *k*-point sampling, 4 × 4 × 4, was carried on numerical integration of the Brillouin zone for $Cs_2VOF_4(IO_2F_2)$.

The calculated band gaps tend to be smaller than the experimental values because of the discontinuous exchange-correlation in the DFT. Therefore, we calculated the imaginary part of the dielectric function according to the electron transition from the valence bands (VB) to the conduction band (CB) based on the electron band structure of the scissor-corrected. Consequently, the real part of the dielectric function was acquired and the calculated refractive index was determined through the Kramers-Kronig transform.[8]

The Birefringence Experiment

The birefringence of $Cs_2VOF_4(IO_2F_2)$ were measured by a Nikon Eclipse polarizing microscope E200MV POL equipped with a visible light filter. According to crystal optics, the retardation is proportional to birefringence and thickness of crystal. The specific formula is $R = \Delta n \times d$, where R, Δn and d represent retardation, birefringence and thickness of crystal, respectively.

Refence

1. *SAINT: Program for Area Detector Absorption Correction, Ver,4.05*; Siemens Analytical X-ray Instruments: Madison, WI, 1995.
2. G. M. Sheldrick, *SHELXTL*, *version 6.12*; Bruker Analytical X-ray Instruments, Inc.: Madison, WI, 2001.
3. S. K. Kurtz and T. T. Perry, *J. Appl. Phys*., 1968, **39**, 3798.
4. M. D. Segall, P. J. D. Lindan, M. J. Probert, C. J. Pickard, P. J. Hasnip, S. J. Clark and M. C. Payne, *J Phys-Condens Mat*., 2002, **14**, 2717–2744.
5. V. Milman, B. Winkler, J. A. White, C. J. Pickard, M. C. Payne, E. V. Akhmatskaya and R. H. Nobes, *Int. J. Quantum Chem*., 2000, **77**, 895–910.
6. J. P. Perdew, K. Burke and M. Ernzerhof, *Phys. Rev. Lett*., 1996, **77**, 3865–3868.
7. J. S. Lin, A. Qteish, M. C. Payne and V. Heine, *Phys Rev B*, 1993, **47**, 4174–4180.
8. E. D. Palik, *J. Opt. Soc. Am. A*., 1984, **1**, 1297–1297.

Table S1. Crystal data and structure refinement for $Cs_2VOF_4(IO_2F_2)$.

Empirical formula	$Cs_2VOF_4(IO_2F_2)$
Formula weight	605.66
Temperature	295(2) K
Crystal system	Orthorhombic
space group	$Cmc2_1$
a/ Å	12.188(2)
b/ Å	10.349(15)
c/ Å	7.779(12)
V/ Å^3	981.2(3)
Z	4
D_{calcd}/ g/cm^3	4.100
Completeness to	100.0%
μ(Mo_Kα)/mm^{-1}	11.535
Flack factor	0.11(7)
GOF on F^2	1.094
Final R indices [F_o^2>2s(F_o^2)][a]	R_1 = 0.0402,
	wR_2 = 0.0508
R indices (all data)	R_1 = 0.0582,
	wR_2 = 0.0567
Absolute structure parameter	0.11(7)
Largest diff. peak and hole (e·Å^3)	1.286 and -1.007

[a] $R_1 = \Sigma||F_o| - |F_c||/\Sigma|F_o|$ and $wR_2 = [\Sigma w(F_o^2 - F_c^2)^2 / \Sigma w F_o^4]^{1/2}$ for $F_o^2 > 2\sigma(F_o^2)$

Table S2. Atomic coordinates (× 10^4) and equivalent isotropic displacement parameters ($A^2 \times 10^3$) for $Cs_2VOF_4(IO_2F_2)$. Ueq is defined as one third of the trace of the orthogonalized U_{ij} tensor.

	x	y	z	U(eq)	BVS
Cs(1)	1947(1)	3412(1)	3578(2)	35(1)	1.07
V(1)	5000	1696(5)	3320(8)	27(1)	5.17
I(1)	5000	4695(2)	6346(3)	25(1)	5.16
O(1)	5000	3765(18)	4410(20)	36(6)	2.05
O(2)	5000	3510(20)	8020(20)	43(7)	2.03
O(3)	5000	310(20)	2450(30)	46(6)	2.01
F(1)	3994(10)	2456(10)	1934(13)	32(3)	1.12
F(2)	6073(10)	1427(14)	4869(16)	43(4)	1.03
F(3)	6645(9)	4664(11)	6380(20)	49(3)	1.03

Table S3. Bond lengths [Å] and angles [deg.] for $Cs_2VOF_4(IO_2F_2)$.

Cs(1)-F(1)	2.973(11)	F(1)-Cs(1)-F(2)#6	133.3(3)
Cs(1)-F(1)#1	2.989(11)	F(1)#1-Cs(1)-F(2)#6	84.2(3)
Cs(1)-F(3)#2	3.060(15)	F(3)#2-Cs(1)-F(2)#6	65.3(3)
Cs(1)-F(2)#3	3.080(12)	F(2)#3-Cs(1)-F(2)#6	96.7(3)
Cs(1)-O(2)#4	3.129(14)	O(2)#4-Cs(1)-F(2)#6	112.5(4)
Cs(1)-F(3)#5	3.138(14)	F(3)#5-Cs(1)-F(2)#6	75.7(3)
Cs(1)-O(3)#6	3.204(14)	O(3)#6-Cs(1)-F(2)#6	45.1(4)
Cs(1)-F(2)#2	3.324(14)	F(2)#2-Cs(1)-F(2)#6	134.1(4)
Cs(1)-F(2)#6	3.447(14)	F(1)-Cs(1)-F(3)#3	65.8(3)
V(1)-O(3)	1.580(2)	F(1)#1-Cs(1)-F(3)#3	96.3(3)
V(1)-F(2)	1.800(12)	F(3)#2-Cs(1)-F(3)#3	139.7(2)
V(1)-F(2)#2	1.800(12)	F(2)#3-Cs(1)-F(3)#3	64.6(4)
V(1)-F(1)	1.813(12)	O(2)#4-Cs(1)-F(3)#3	45.5(3)
V(1)-F(1)#2	1.813(12)	F(3)#5-Cs(1)-F(3)#3	110.7(4)
V(1)-O(1)	2.303(19)	O(3)#6-Cs(1)-F(3)#3	109.6(4)
I(1)-O(2)	1.784(19)	F(2)#2-Cs(1)-F(3)#3	71.0(3)
I(1)-O(1)	1.787(18)	F(2)#6-Cs(1)-F(3)#3	154.1(3)
I(1)-F(3)#2	2.006(11)	F(1)-Cs(1)-O(1)	44.2(3)
I(1)-F(3)	2.006(11)	F(1)#1-Cs(1)-O(1)	104.8(4)
F(1)-Cs(1)-F(1)#1	126.7(2)	F(3)#2-Cs(1)-O(1)	44.6(4)
F(1)-Cs(1)-F(3)#2	88.6(3)	F(2)#3-Cs(1)-O(1)	119.6(4)
F(1)#1-Cs(1)-F(3)#2	73.8(3)	O(2)#4-Cs(1)-O(1)	145.9(5)
F(1)-Cs(1)-F(2)#3	84.5(3)	F(3)#5-Cs(1)-O(1)	59.7(3)
F(1)#1-Cs(1)-F(2)#3	134.6(3)	O(3)#6-Cs(1)-O(1)	135.5(4)
F(3)#2-Cs(1)-F(2)#3	146.9(4)	F(2)#2-Cs(1)-O(1)	45.3(4)
F(1)-Cs(1)-O(2)#4	111.4(4)	F(2)#6-Cs(1)-O(1)	99.6(3)
F(1)#1-Cs(1)-O(2)#4	68.9(4)	O(3)-V(1)-F(2)	98.4(7)
F(3)#2-Cs(1)-O(2)#4	142.6(4)	O(3)-V(1)-F(2)#2	98.4(7)
F(2)#3-Cs(1)-O(2)#4	69.0(4)	F(2)-V(1)-F(2)#2	93.2(9)
F(1)-Cs(1)-F(3)#5	61.1(3)	O(3)-V(1)-F(1)	98.0(7)
F(1)#1-Cs(1)-F(3)#5	151.3(3)	F(2)-V(1)-F(1)	163.1(7)
F(3)#2-Cs(1)-F(3)#5	79.21(19)	F(2)#2-V(1)-F(1)	88.5(5)
F(2)#3-Cs(1)-F(3)#5	69.1(4)	O(3)-V(1)-F(1)#2	98.0(7)
O(2)#4-Cs(1)-F(3)#5	138.0(4)	F(2)-V(1)-F(1)#2	88.5(5)
F(1)-Cs(1)-O(3)#6	135.1(4)	F(2)#2-V(1)-F(1)#2	163.1(7)
F(1)#1-Cs(1)-O(3)#6	98.0(4)	F(1)-V(1)-F(1)#2	85.1(8)
F(3)#2-Cs(1)-O(3)#6	110.4(4)	O(3)-V(1)-O(1)	176.4(10)
F(2)#3-Cs(1)-O(3)#6	57.0(4)	F(2)-V(1)-O(1)	84.1(6)
O(2)#4-Cs(1)-O(3)#6	78.0(4)	F(2)#2-V(1)-O(1)	84.1(6)
F(3)#5-Cs(1)-O(3)#6	82.3(4)	F(1)-V(1)-O(1)	79.4(5)
F(1)-Cs(1)-F(2)#2	46.8(3)	F(1)#2-V(1)-O(1)	79.4(5)
F(1)#1-Cs(1)-F(2)#2	80.2(3)	O(2)-I(1)-O(1)	104.2(8)
F(3)#2-Cs(1)-F(2)#2	68.9(3)	O(2)-I(1)-F(3)#2	88.9(4)

F(2)#3-Cs(1)-F(2)#2	124.6(3)	O(1)-I(1)-F(3)#2	90.1(5)
O(2)#4-Cs(1)-F(2)#2	101.5(4)	O(2)-I(1)-F(3)	88.9(4)
F(3)#5-Cs(1)-F(2)#2	99.2(3)	O(1)-I(1)-F(3)	90.1(5)
O(3)#6-Cs(1)-F(2)#2	178.1(4)	F(3)#2-I(1)-F(3)	177.8(8)

Symmetry transformations used to generate equivalent atoms:
#1 -x+1/2,-y+1/2,z+1/2 #2 -x+1,y,z #3 x-1/2,-y+1/2,z-1/2 #4 -x+1/2,-y+1/2,z-1/2 #5 -x+1,-y+1,z-1/2 #6 x-1/2,y+1/2,z #7 -x+1/2,y-1/2,z #8 x+1/2,y-1/2,z #9 x+1/2,-y+1/2,z-1/2 #10 x+1/2,-y+1/2,z+1/2 #11 -x+1,-y+1,z+1/2

Table S4. Investigation of reported ETM iodates and F-containing ETM iodates with MO_6 octahedra in Figure 2.

Ratio	Compounds	Space group	Dimension	BBUs	SHG	Phase matching behavior	Lewis acid strengths of A-site cations
	ETM iodates						
/	$KMoO_3(IO_3)$	*Pbca*	2D	$[MoO_4(IO_3)_2]^{4-}$ cluster	CS	/	0.111
/	$AMoO_3(IO_3)$ (A= Rb, Cs)	$Pna2_1$	3D	$[MoO_4(IO_3)_2]^{4-}$ cluster	400×SiO_2	PM	0.111
/	$A[(VO)_2(IO_3)_3O_2]$ (A=Rb,Cs,NH_4)	*Ima*2	1D	$[VO_2(IO_3)_2]^-$ chain	500×SiO_2	PM	0.100
/	$A_2Ti(IO_3)_6$ (A=Li, Na)	$P6_3$	0D	$[Ti(IO3)6]^{2-}$ cluster	600,400×SiO_2	PM	0.167
	$A_2Ti(IO_3)_6$ (A= K, Rb, Cs, Tl)	$R\bar{3}$	0D	$[Ti(IO3)6]^{2-}$ cluster	CS	/	0.111
/	$BaNbO(IO_3)_5$	*Cc*	0D	$[NbO(IO_3)_5]^{2-}$ cluster	14 × KDP	PM	0.200
/	$NaVO_2(IO_3)_2(H_2O)$	$P2_1$	2D	$[(VO_2)(IO_3)_2]^-$ chain	20 × KDP	PM	0.167
/	$K(VO)_2O_2(IO_3)_3$	*Ima*2	1D	$[VO_2(IO_3)_2]^-$ chain	3.6 × KTP	PM	0.125
	F-containing ETM iodates with MO_6 octahedron						
I/ETM> 1	α, β-$Ba[VFO_2(IO_3)_2]$	*α-Pbcn* *β-*$P2_12_12_1$	0D	$[VFO_2(IO_3)_2]^{2-}$ cluster	*α*-CS *β*-1.5×KDP	/ PM	0.182-0.200
	α, β-$Ba_2[VO_2F_2(IO_3)_2]IO_3$	*α-*$Pna2_1$ *β-*$P2_1$	0D	$[VO_2F_2(IO_3)_2]^{3-}$ cluster	9 × KDP	PM	0.182
	$K_3V_2O_3F_4(IO_3)_3$	$Cmc2_1$	0D	$[V_2O_3F_4(IO_3)_3]^{3-}$ cluster	1.3 × KTP	PM	0.125-0.143
I/ETM< 1	$K_5(W_3O_9F_4)(IO_3)$	*Pm*	1D	$[W_3O_{12}F_4]^{10-}$ chain	11 × KDP	PM	0.125-0.200
	$Ba_2[MoO_3F(IO_3)](MoO_3F_2)$	*Cc*	1D	$[MoO_3F(IO_3)]^{2-}$ chain	8 × KDP	PM	0.167-0.200
I/ETM= 1	$CsVO_2F(IO_3)$	$Pna2_1$	3D	$[VO_2F(IO_3)_2]^{2-}$ chain	1.1 × KTP	PM	0.100
	$A_2MoO_2F_3(IO_2F_2)$ (A= Rb, Cs)	$Cmc2_1$	0D	$[MoO_2F_3(IO_2F_2)]^{2-}$ cluster	5 × KDP 4.5× KDP	PM	0.100
	$Cs_2VOF_4(IO_2F_2)$(This work)	$Cmc2_1$	0D	$[VOF_4(IO_2F_2)]^{2-}$ cluster	5 × KDP	PM	0.111

Table S5. The residual negative charges of O/F atoms in M-O/F and I-O/F bonds.

MO_6 and IO_3	Bond	R_o (Å)	S_i	V-S_i	Lewis base strengths of anions group
$[MoO_6]^{6-}$	Mo-O	1.907	1.00	1.000	0.333
using F^- to substitute O^{2-}	Mo-F	1.821	1.00	0	0
$[WO_6]^{6-}$	W-O	1.917	1.00	1.000	0.333
	W-F	1.836	1.00	0	0
$[VO_6]^{7-}$	V-O	1.803	0.833	1.167	0.389
	V-F	1.709	0.833	0.167	0.083
$[NbO_6]^{7-}$	Nb-O	1.911	0.833	1.167	0.389
	Nb-F	1.870	0.833	0.167	0.083
$[TaO_6]^{7-}$	Ta-O	1.920	0.833	1.167	0.389
	Ta-F	1.880	0.833	0.167	0.083
$[TiO_6]^{8-}$	Ti-O	1.815	0.667	1.333	0.444
	Ti-F	1.756	0.667	0.333	0.167
$[ZrO_6]^{8-}$	Zr-O	1.928	0.667	1.333	0.444
	Zr-F	1.846	0.667	0.333	0.167
$[IO_3]^-$	I-O	2.003	1.667	0.333	0.111
	I-F	1.910	0.767	0.233	0.042

Table S6. The directions and magnitudes of the dipole moments in $[IO_2F_2]^-$ and $[VO_2F_4]^{3-}$ polyhedra.

	x	y	z	Total (Debye)
IO_2F_2	0	0	-17.958	-17.958
VO_2F_4	0	0	0.676	0.676
Total	0	0	-17.282	-17.282

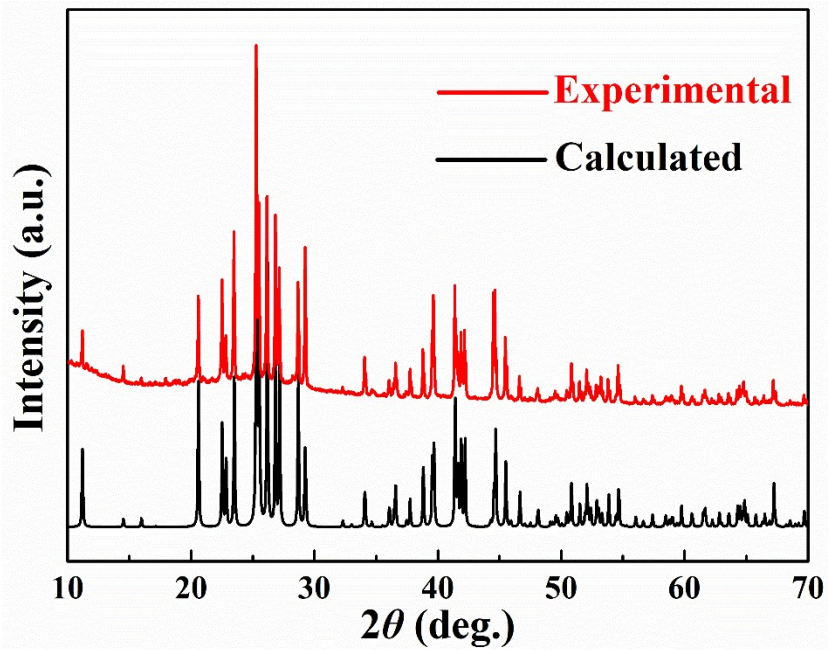

Figure S1. Experimental and calculated PXRD patterns of $Cs_2VOF_4(IO_2F_2)$.

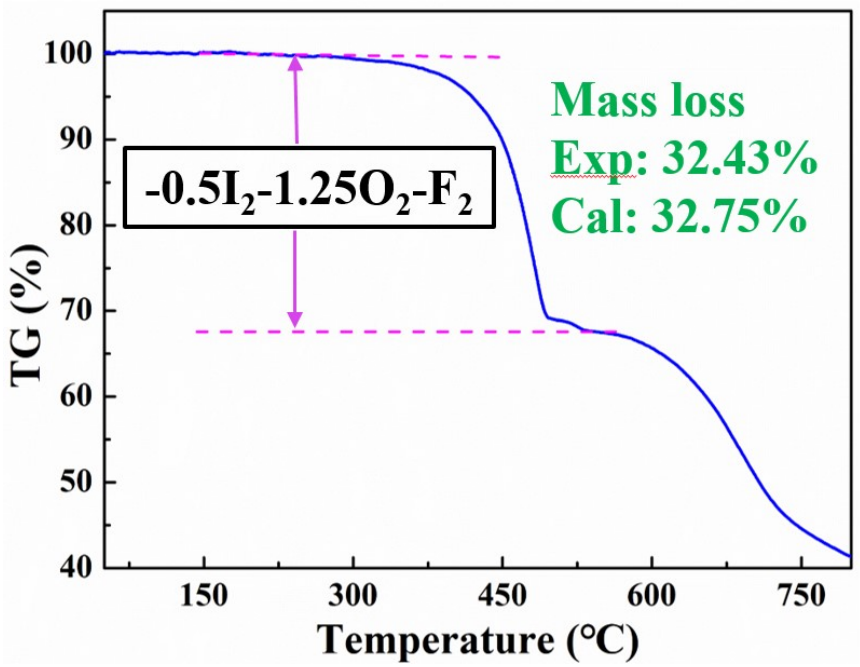

Figure S2. TG curve of $Cs_2VOF_4(IO_2F_2)$.

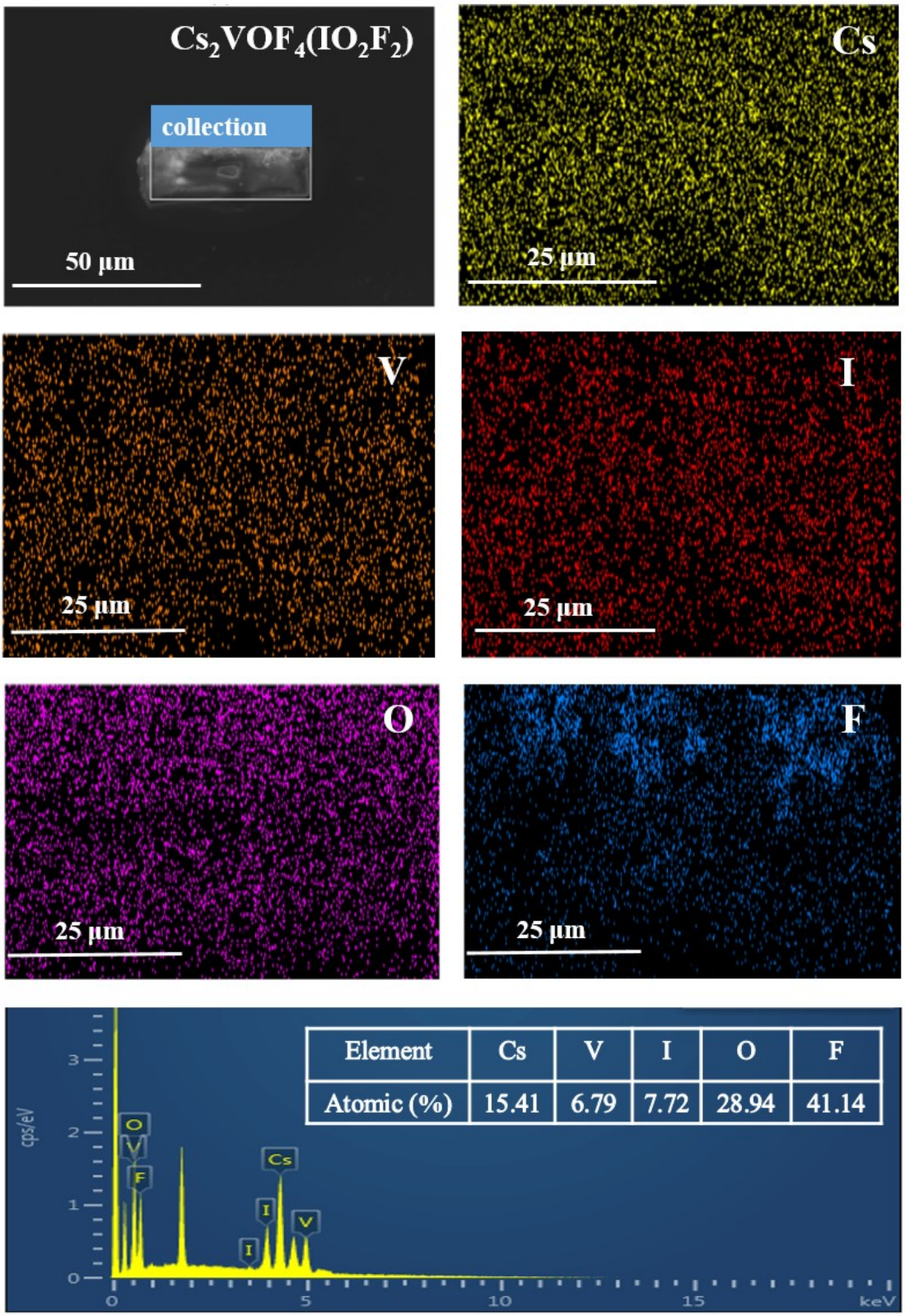

Element	Cs	V	I	O	F
Atomic (%)	15.41	6.79	7.72	28.94	41.14

Figure S3. The elemental analysis of $Cs_2VOF_4(IO_2F_2)$.

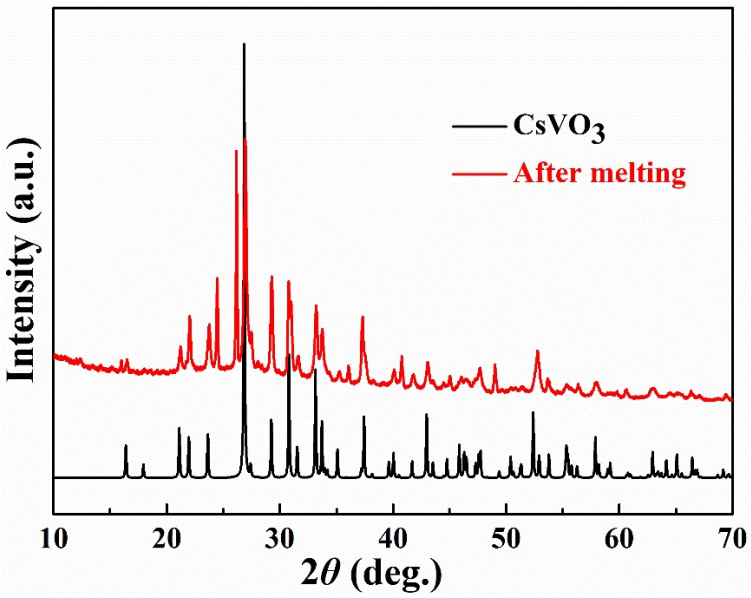

Figure S4. The residual PXRD patterns of $Cs_2VOF_4(IO_2F_2)$.

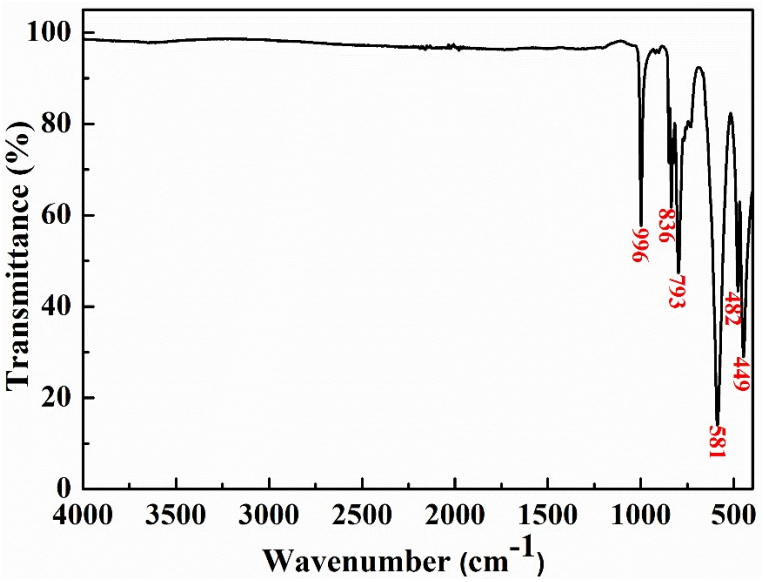

Figure S5. IR transmission spectrum of $Cs_2VOF_4(IO_2F_2)$.

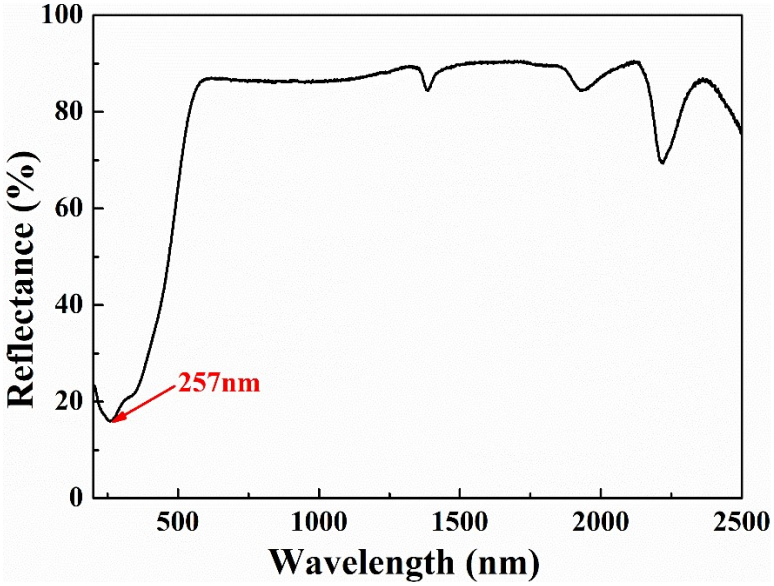

Figure S6. Diffuse reflectance spectrum of $Cs_2VOF_4(IO_2F_2)$.

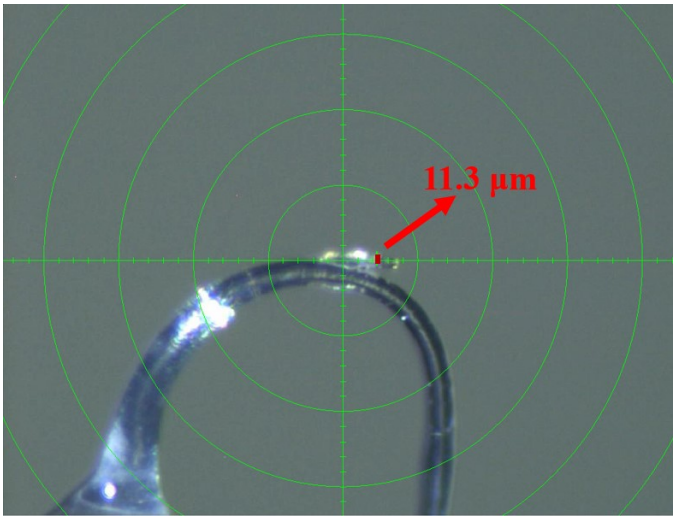

Figure S7. The photo of crystal size for measuring birefringence of $Cs_2VOF_4(IO_2F_2)$.